PHYSICAL REVIEW B VOLUME 28, NUMBER 8 15 OCTOBER 1983

Hydrogenic-impurity ground state in GaAs-$Ga_{1-x}Al_xAs$ multiple–quantum-well structures

S. Chaudhuri
University Research Center, Wright State University, Dayton, Ohio 45435
(Received 21 March 1983)

We report the results of a variational calculation for the hydrogenic-impurity ground state in a multiple–quantum-well structure consisting of alternating slabs of GaAs and $Ga_{1-x}Al_xAs$. Calculations have been carried out with the assumption that the impurity envelope wave function spreading beyond the next-nearest-neighbor GaAs wells is negligible. Impurity envelope wave functions have been plotted for some typical GaAs well and $Ga_{1-x}Al_xAs$ barrier thicknesses to find the extent of wave-function spreading. The binding energy is found to vary substantially as a function of the barrier thickness. Calculations are performed for the variations of the binding energy as a function of the well thickness and also as a function of the barrier thickness. The main peak in the impurity binding energy in superlattices with equal well and barrier thickness is shifted towards a thickness larger than that in single-well systems. A secondary peak appears at a very small thickness, which arises because the model includes only three wells. The results of the present calculation in various limiting cases agree with previous results.

I. INTRODUCTION

The recent advances in crystal-growth techniques such as molecular-beam epitaxy and metal-organic chemical-vapor deposition (MOCVD) have made possible the growth of systems consisting of alternate layers of two different lattice-matched semiconductors with very precisely controlled thicknesses and sharp interfaces. Such one-dimensional periodic structures are generally referred to as superlattices. Numerous studies have been devoted to various aspects of the electronic states associated with such systems.[1] Among the superlattices grown, so far, the GaAs-$Ga_{1-x}Al_xAs$ system is the simplest and the most extensively studied. The band gap of $Ga_{1-x}Al_xAs$ increases with the concentration x of aluminum. Thus there exists a discontinuity of the band edges at the GaAs-$Ga_{1-x}Al_xAs$ interfaces. The conduction-band-edge discontinuity is about 85% of ΔE_g; the band-gap difference between bulk $Ga_{1-x}Al_xAs$ and GaAs. The valence-band-edge discontinuity is about 15% of ΔE_g. As a result, the electrons and holes in a GaAs layer find themselves in approximately rectangular potential wells for sharp interfaces.

Studies of the shallow impurity states in such quantum wells have recently begun with the work of Bastard.[2] He calculated the ground-state binding energy of a hydrogenic shallow impurity in the GaAs quantum well. In that calculation the potential barrier height in the $Ga_{1-x}Al_xAs$ regions was taken to be infinite. He finds that the binding energy increases as the well size (i.e., the GaAs layer thickness) is reduced. Mailhiot, Chang, and McGill[1] (MCM) have done an extensive calculation for the binding energies, wave functions, and their variations with well thickness, impurity position, etc., for realistic finite potential-barrier height, contrary to Bastard's infinite barrier height. They also include the effects due to different effective electronic masses and dielectric constants in GaAs and $Ga_{1-x}Al_xAs$ layers. They have found that the binding energy goes through a maximum as the well size is reduced instead of continuously increasing as is found in the infinite-barrier calculation. Greene and Bajaj[3] (GB) have also performed a similar calculation for impurities at the center of a quantum well. Both of the groups, MCM and GB, have calculated some excited-state binding energies.

In all of the previous calculations it has been assumed that the $Ga_{1-x}Al_xAs$ layers are thick enough to confine the wave functions so that they do not spill over to the adjacent GaAs quantum wells. Calculations were performed with this assumption for an impurity in a quantum well with two semi-infinite $Ga_{1-x}Al_xAs$ barriers on each side of the well. Superlattices are made with layer thickness ranging from a few monolayers to about 400 Å. Most attention has been focused on systems with aluminum concentration x of $Ga_{1-x}Al_xAs$ less than 0.45. In this concentration range the band gap is direct at the Γ point.[4] The spreading of the impurity envelope wave functions depends on the potential barrier height as well as the barrier thickness. In general wave functions spread more to the adjacent wells if the barrier height or the thickness is reduced. Thus the previous calculations with single-well approximation are not adequate for thin superlattices, or even for moderately thick superlattices but with small aluminum concentrations. This is evident from the wave-function plot of MCM.[1] In this situation we feel that it is desirable to perform a calculation which should be valid for thin or small barrier-height superlattices. The present paper, to our knowledge, is the first report of such a calculation. In this calculation we consider for simplicity the impurity to be at the center of a well. Assuming that the spread of the wave functions to the next-nearest-neighbor wells of the one containing the impurity, the calculation has been performed with only one well on each side of the well under consideration. Wave functions have been plotted along the axis of the superlattice to see the extent of wave-function penetration into the next-nearest-

wells and barriers. These plots are intended to give a feeling for how thin a superlattice the present model may be valid.

In Sec. II we derive the spectrum of the impurity ground-state energy with respect to the lowest subband in a multiple–quantum-well structure. Main results are presented in Sec. III. A summary and discussion of the results are presented in Sec. IV.

II. GROUND-STATE ENERGY CALCULATION IN A MULTIPLE–QUANTUM-WELL

Let us for definiteness consider a donor impurity atom at the center of a quantum well of thickness $L=2a$. The calculation may be valid for hydrogenic acceptor states as well in an approximate way since the valence-band degeneracy in GaAs is lifted by the presence of the barriers. Although for a complete calculation for acceptor states a multiband effective-mass calculation may be necessary. We consider impurities which may be described by the hydrogenic–effective-mass theory (HEMT). A detailed discussion on the validity of HEMT in bulk materials has been given by Pantelides.[5] For shallow donor states in GaAs, HEMT is known to be valid to a high degree of accuracy. We assume that the spread of the impurity envelope wave functions to the next-nearest-neighbor quantum wells is negligible. Thus we consider the following model for the periodic potential along the axis (z axis) normal to the interfaces of the superlattice with sharp interfaces (see Fig. 4):

$$V(z)=\begin{cases} V_0 & \text{if } a<|z|<a+b \text{ or } 3a+b<|z|<\infty \\ 0 & \text{if } 0<|z|<a \text{ or } a+b<|z|<3a+b \end{cases} . \tag{1}$$

The GaAs well thickness is $2a$ and the $Ga_{1-x}Al_xAs$ barrier thickness is b. The barrier height V_0 is obtained from the 85% (15%) rule[4] of the band-gap discontinuity ΔE_g for donor (acceptor) states for aluminum concentration $x \lesssim 0.45$, such that the band gap is direct at the Γ point and ΔE_g is given by[6]

$$\Delta E_g = 1.155x + 0.37x^2 , \tag{2}$$

in eV. According to HEMT the Hamiltonian for the impurity at the center of a quantum well in a superlattice is

$$H = -\nabla^2 - \frac{e^2}{2r} + V(z) . \tag{3}$$

The Hamiltonian is written in a dimensionless form so that all energies are measured in units of the effective Rydberg $R^* = m^* e^4/2\hbar^2\epsilon^2$ and all distances are measured in units of the effective Bohr radius $a^* = \hbar^2\epsilon/m^* e^2$, where m^* and ϵ are the electronic effective mass and the dielectric constant, respectively, of GaAs. There are slight differences in the effective masses and dielectric constants of GaAs and $Ga_{1-x}Al_xAs$. Note that we have neglected these small differences in the Hamiltonian. Since the impurity binding energies are measured with respect to the lowest subband energy we need to solve for the ground-state energy corresponding to the Hamiltonian given by Eq. (1) without the Coulomb term. Since H is even under reflection against the x-y plane, for the impurity at the center, parity is conserved. We are interested in the ground-state energy. So we consider the even-parity solution of H without the Coulomb term. This may be written as

$$\Psi_s = \begin{cases} \cos\alpha z & \text{if } 0<z<a \\ Ae^{\beta z}+Be^{-\beta z} & \text{if } a<z<a+b \\ C\cos\alpha z + D\sin\alpha z & \text{if } a+b<z<3a+b \\ Fe^{-\beta z} & \text{if } 3a+b<z<\infty . \end{cases} \tag{4}$$

The quantities α and β are given by

$$\alpha=\sqrt{E_0} \text{ and } \beta=\sqrt{E_0-V_0} , \tag{5}$$

where E_0 is the eigenenergy of an electron in the potential given by Eq. (1). By matching the wave function at the interfaces $z=a$, $a+b$, and $3a+b$, the eigenenergies E_0 can be shown to be given by the solution of the transcendental equation

$$\alpha\tan(\alpha a)=\beta' , \tag{6}$$

where

$$\beta' = \beta\frac{Be^{-\beta a}-Ae^{\beta a}}{Be^{-\beta a}+Ae^{\beta a}} .$$

The smallest solution E_0 of Eq. (6) gives the lowest subband energy. To solve for E_0 we have to know the ratio of the coefficients A and B in terms of α and β. They are obtained from the wave function and its derivative matching at the interfaces and are given explicitly in the Appendix. At this point it may be pointed out that these simple matching conditions are valid for simple superlattices like GaAs-$Ga_{1-x}Al_xAs$.[7,8] For other superlattices like GaSb-InAs, where there is a common energy region between the conduction band of one material and the valence band of the other, or where there is a large difference in the two material parameters, more complex matching conditions as well as wave functions may become necessary.[9] In the limiting case of $b\to\infty$, it can be easily shown that Eq. (1) reduces to the well-known transcendental equation $\alpha\tan\alpha a=\beta$ for a square well. In the other limiting case of $b\to 0$, Eq. (6) reduces correctly to $\alpha\tan 3\alpha a=\beta$, which corresponds to a well of thickness equal to 3 times that of a single well. Once E_0 is known, the coefficients A, B, C, D, and F (and hence Ψ_s) are known. These are also written down in the Appendix.

Following Bastard's procedure for a single infinite quantum well we consider the trial function for the ground state of the full Hamiltonian H as

$$\Psi = N\Psi_s\Psi_c , \tag{7}$$

with

$$\Psi_c = e^{-r/\lambda} ,$$

where λ is the single variational parameter and N is the normalization constant. Ψ_s is the ground-state eigenfunction of H without the Coulomb potential and Ψ_c is the ground-state eigenfunction of H without $V(z)$. The variational ground-state binding energy $E(a,b)$ is given by

$$E = E_0 - \min\langle\Psi|H|\Psi\rangle . \tag{8}$$

The normalization constant N and the expectation values of the operators of H are as follows:

$$N=\frac{1}{\sqrt{2\pi}}[I_0(0)+I_0(\alpha)+2A^2J_1(\beta)+2B^2J_1(-\beta)+4ABJ_1(0)+(C^2+D^2)I_2(0)+(C^2-D^2)I_2(\alpha)$$
$$+2CDK_2(\alpha)+2F^2J_3(-\beta)]^{-1/2}\,, \tag{9a}$$

$$\langle\Psi|-\nabla^2|\Psi\rangle=1/\lambda^2+2\pi N^2(\alpha^2[I_0(0)-I_0(\alpha)]+2\beta^2[A^2J_1(\beta)+B^2J_1(-\beta)-2ABJ_1(0)]$$
$$+\alpha^2[(C^2+D^2)I_2(0)+(D^2-C^2)I_2(\alpha)-2CDK_2(\alpha)]+2\beta^2F^2J_3(-\beta)$$
$$+\frac{2}{\lambda}\{\alpha M_0(\alpha)-2\beta[A^2P_1(\beta)-B^2P_1(-\beta)]$$
$$-\alpha[(D^2-C^2)M_2(\alpha)+2CDL_2(\alpha)]+2\beta F^2P_3(-\beta)\})\,, \tag{9b}$$

$$\langle\Psi|(-2/r)|\Psi\rangle=-4\pi N^2[Q_0(0)+Q_0(\alpha)+2A^2S_1(\beta)+2B^2S_1(-\beta)+4ABS_1(0)+(C^2+D^2)Q_2(0)$$
$$+(C^2-D^2)Q_2(\alpha)+2CDR_2(\alpha)+2F^2S_3(-\beta)]\,, \tag{9c}$$

$$\langle\Psi|V(z)|\Psi\rangle=4\pi N^2V_0[A^2J_1(\beta)+B^2J_1(-\beta)+2ABJ_1(0)+F^2J_3(-\beta)]\,. \tag{9d}$$

The integrals $I_n(\alpha)$, $J_n(\beta)$, $K_n(\alpha)$, $I_m(\alpha)$, $M_n(\alpha)$, $P_n(\beta)$, $Q_n(\alpha)$, $R_n(\alpha)$, and $S_n(\beta)$ are defined in the Appendix. The subscripts of the integrals denote the region of integration. The subscript "0" stands for the central half-well ($0\rightarrow a$), 1 stands for the region a to $a+b$, 2 for $a+b$ to $3a+b$, and 3 for $3a+b$ to ∞.

In the single–quantum-well limit (i.e., $b\rightarrow\infty$), the quantities of Eq. (9) reduce to the following explicit forms:

$$N=(2/\pi\lambda^3)^{1/2}\left\{1+\frac{1}{(1+\alpha^2\lambda^2)^2}-e^{-2a/\lambda}\left[1+\frac{a}{\lambda}+\frac{\cos(2\alpha a)}{(1+\alpha^2\lambda^2)}\left[\frac{a}{\lambda}+\frac{1}{1+\alpha^2\lambda^2}\right]-\frac{\alpha\lambda\sin(2\alpha a)}{2(1+\alpha^2\lambda^2)}\left[1+\frac{2a}{\lambda}+\frac{2}{1+\alpha^2\lambda^2}\right]\right.\right.$$
$$\left.\left.-\frac{\cos^2(\alpha a)}{1+\beta\lambda}\left[1+\frac{2a}{\lambda}+\frac{1}{1+\beta\lambda}\right]\right]\right\}^{-1/2}\,, \tag{10a}$$

$$\langle\Psi|-\nabla^2|\Psi\rangle=\frac{1}{\lambda^2}+\alpha^2-\frac{\pi N^2\alpha\lambda^2}{2}e^{-2a/\lambda}\left[1+\frac{2a}{\lambda}\right]\sin(2\alpha a)$$
$$+\frac{\pi N^2\lambda}{2}\cos^2(\alpha a)e^{-2a/\lambda}\left[1+(\beta+1/\lambda)2a+\frac{\beta^2-\alpha^2}{\beta\lambda+1}\lambda^2-\frac{1+\alpha^2\lambda^2}{(1+\beta\lambda)^2}-\frac{(1+\alpha^2\lambda^2)}{1+\beta\lambda}\frac{2a}{\lambda}\right]\,, \tag{10b}$$

$$\langle\Psi|(-2/r)|\Psi\rangle=-\pi N^2\lambda^2\left[1+\frac{1}{1+\alpha^2\lambda^2}-e^{-2a/\lambda}\left[1+\frac{\cos(2\alpha a)}{1+\alpha^2\lambda^2}-\frac{\alpha\sin(2\alpha a)}{\lambda(1+\alpha^2\lambda^2)}\right]+\frac{2\beta^2}{1+\beta\lambda}e^{-2(\beta+1/\lambda)a}\right]\,, \tag{10c}$$

$$\langle\Psi|V(z)|\Psi\rangle=\frac{\pi N^2\lambda^3\cos^2(\alpha a)}{2(\beta\lambda+1)}e^{-2a/\lambda}V_0\left[1+\frac{2a}{\lambda}+\frac{1}{1+\beta\lambda}\right]\,. \tag{10d}$$

From Eq. (10) it can be easily shown that in the limit of infinite barrier height (i.e., $V_0\rightarrow\infty$) the normalization constant and the expectation value for the Hamiltonian reduce correctly to the corresponding expressions obtained by Bastard.[2] Now, for the general case of multiple-quantum wells, $\langle\Psi|H|\Psi\rangle$ can be easily computed from Eq. (9) and its minimization with respect to λ leads to the desired binding energy through Eq. (8).

III. RESULTS

We display results for two barrier heights corresponding to aluminum concentrations $x=0.1$ and 0.4. Figure 1 shows the binding energy as a function of the barrier thickness b, with the well thickness L as a parameter. Here we present a physical argument towards the understanding of the behavior of the binding energy as a function of b. We remind the reader that the variational ground-state binding energy is the difference between the lowest eigenvalue E_0 without the impurity potential and the variational energy E_1 (=min. $\langle\Psi|H|\Psi\rangle$). If the wave function is squeezed towards the impurity ion, both E_0 and E_1 increase, but the increase in E_1 would be less than the increase in E_0 due to the attractive Coulomb potential in H. Thus an increase in the barrier thickness from zero tends to more strongly localize the wave function around the impurity ion and thereby increases the binding energy.[2] On the other hand, for finite barrier height V_0, increase in the barrier thickness from zero adds a repulsive term in the energy due to the wave-function penetration in the barrier thus reducing the binding energy. The relative magnitudes of these two competing effects, which depend on the values of L and V_0, determine the behavior of E as a function of b. If the wave function

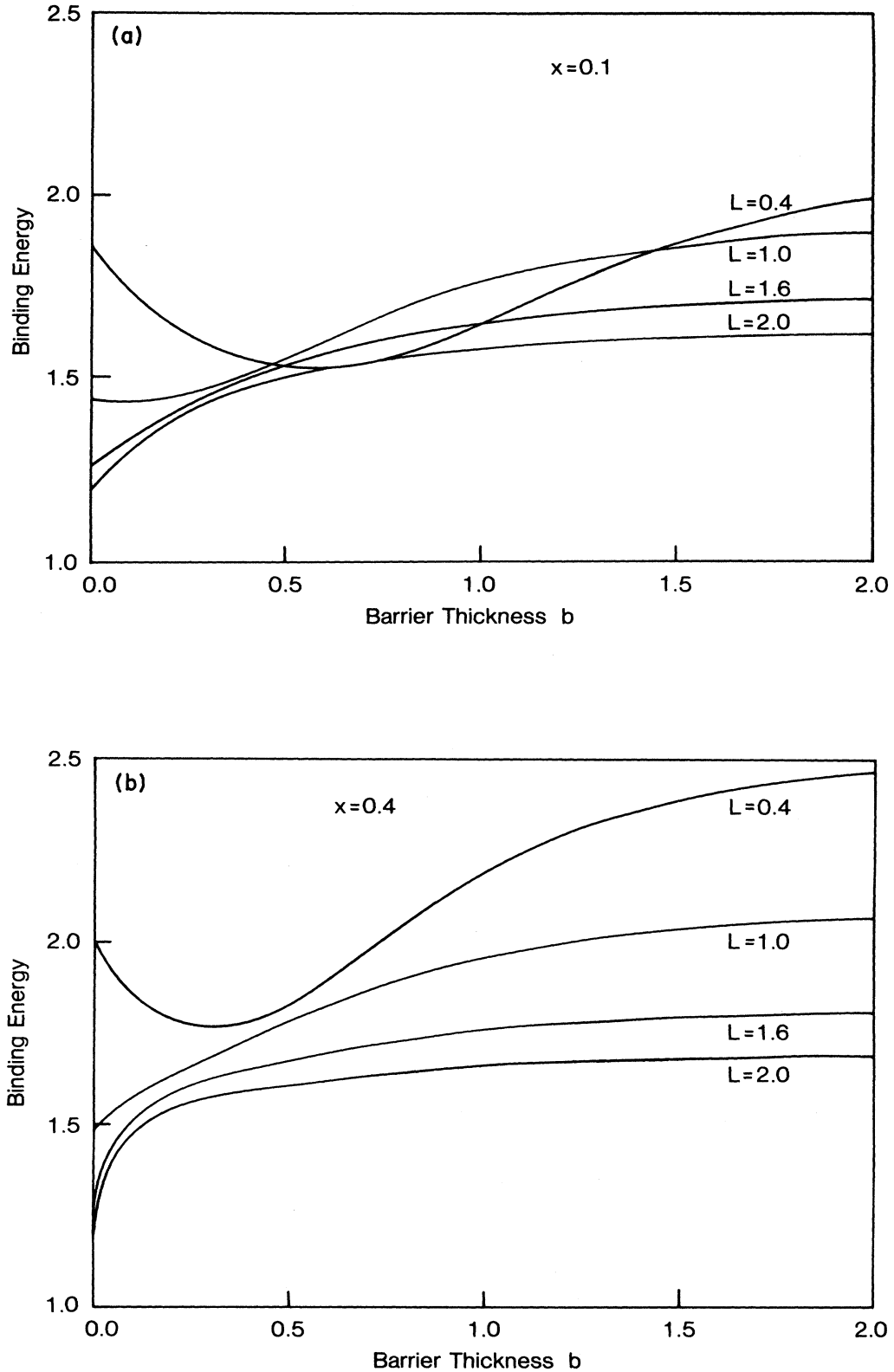

FIG. 1. Binding energy for the hydrogenic-impurity ground state as a function of the $Ga_{1-x}Al_xAs$ layer thickness b for four GaAs layer thicknesses. (a) and (b) are for the alloy compositions $x=0.1$ and 0.4, respectively, of $Ga_{1-x}Al_xAs$. All energies are expressed in terms of the effective Rydberg (R^*) and all distances are expressed in terms of the effective Bohr radius (a^*). Same units are used in all of the following figures.

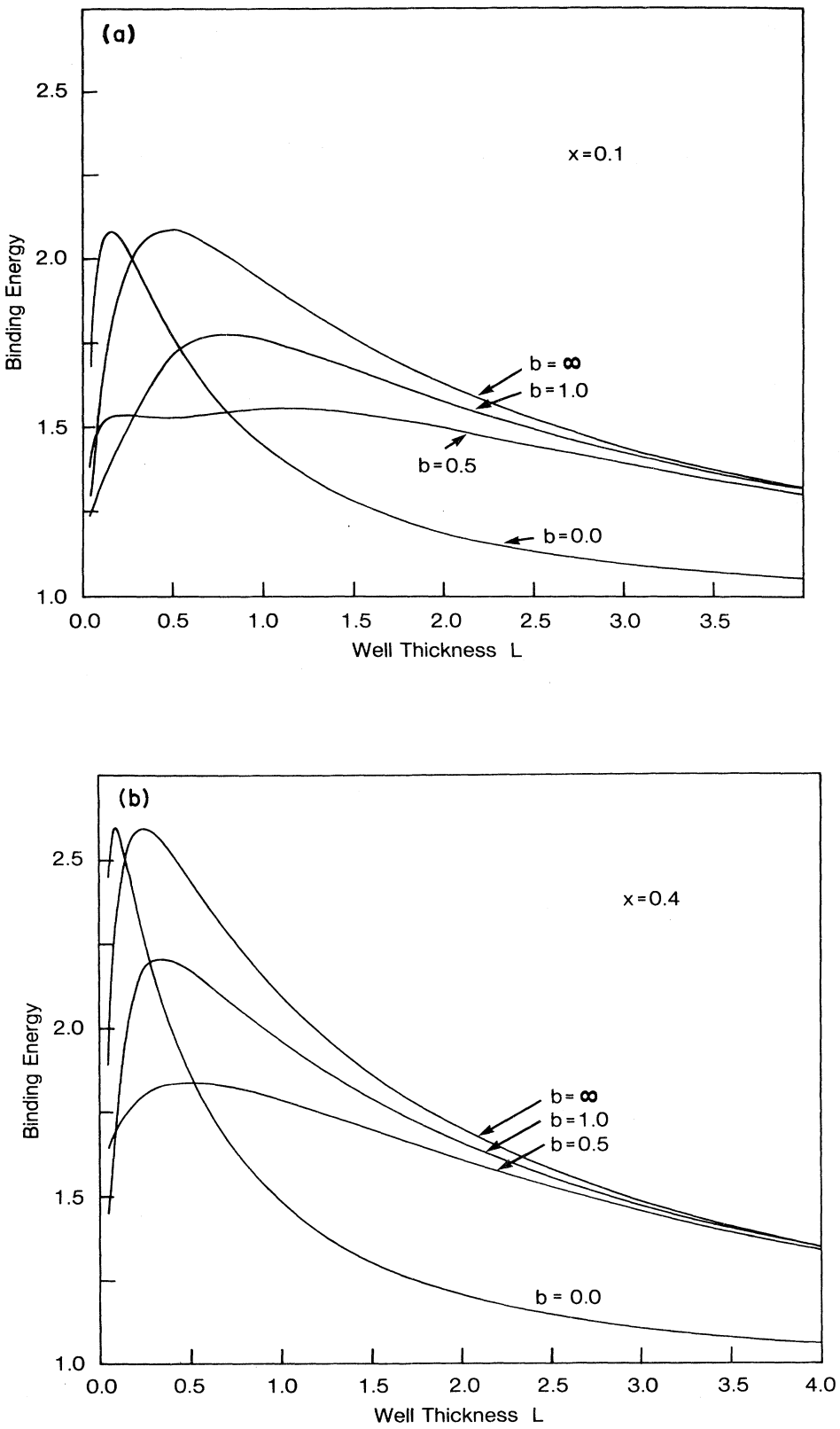

FIG. 2. Binding energy for the hydrogenic-impurity ground state as a function of the GaAs layer thickness for four $Ga_{1-x}Al_xAs$ layer thicknesses. (a) and (b) are for the alloy compositions $x=0.1$ and 0.4, respectively, of $Ga_{1-x}Al_xAs$.

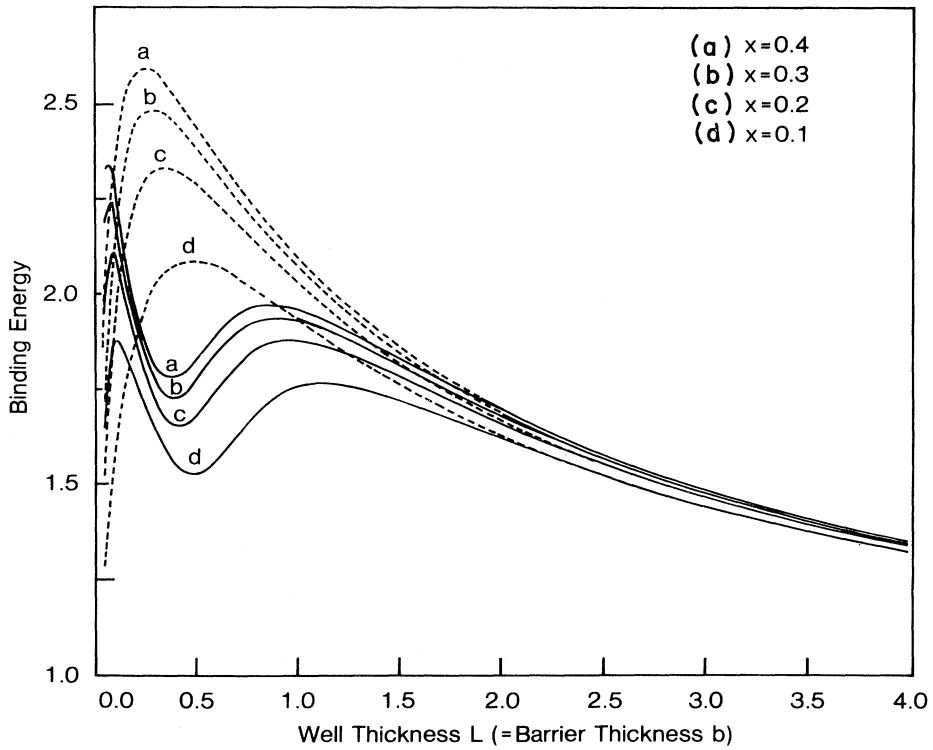

FIG. 3. Binding energy for the hydrogenic-impurity ground state as a function of the GaAs layer thickness when the GaAs and $Ga_{1-x}Al_xAs$ layer thicknesses are equal for alloy compositions $x=0.1$, 0.2, 0.3, and 0.4 of $Ga_{1-x}Al_xAs$.

is already strongly localized around the impurity (e.g., when L is small), the repulsive term added in the energy due to an increase in b is more than the small increase in binding due to further localization of the wave function. Of course, when b is large enough it helps in more localization, and the binding energy increases again approaching the value corresponding to a single-quantum well. This is exactly what we see in Fig. 1. For large well thickness, since there is very little localization, an increase in b always increases the binding energy. Thus there is no valley in the curves for larger L values. Note that in Fig. 1(b) ($V_0 \sim 76R^*$), the minimum of the curve corresponding to $L=0.4$ occurs at a smaller b value than the corresponding curve of Fig. 1(a) ($V_0 \sim 17R^*$). Also for $L=1$, binding energy corresponding to the curve of $x=0.4$ increases monotonically with b unlike the corresponding curve for $x=0.1$ These observations are understandable from the argument given above.

Figures 2(a) and 2(b) present the binding energy as a function of the well thickness with the barrier thickness as a parameter for $x=0.1$ and 0.4, respectively. As mentioned earlier, the limiting case of $b \to 0$ is just the case of a single-quantum well with the well thickness being equal to $3L$. The other limiting case of $b \to \infty$ also becomes a single well with thickness L. An inspection shows that the $b=\infty$ curve can be obtained from the $b=0$ curve by threefold expansion of the abscissa of the latter. A dip in the curve for $b=0.5$ is again in accordance with the argument given in the previous paragraph.

Figure 3 presents the binding energy as a function of the well thickness equal to the barrier thickness with the alloy composition as a parameter. This figure shows interesting results for superlattices with equal well and barrier thicknesses. The dotted lines represent the binding energies corresponding to a single-quantum well. We note that the binding energies obtained from the present calculation exhibit minima at around the well thickness where single-well energies have maxima. By the same argument given before, this type of general behavior is expected since the single-well wave functions are most strongly localized for the well thickness corresponding to maximum binding. The primary peak is shifted towards a thickness larger than that in the single-well system. The other maxima at very small thickness values are due to the fact that in our model we have assumed semi-infinite barriers beyond the adjacent wells. These secondary maxima are not expected to occur in very thin real superlattices with a large number of alternating layers.

Figures 4(a) and 4(b) show the wave functions for $L=b=0.5$ and 0.1, respectively. An inspection of the wave functions shows the validity of our simple model for the multiple—quantum-well systems, at least up to the dimensions $L=b=0.5$, since the wave functions do not spread to the next-nearest-neighbor wells. For very thin superlattices ($L \sim 0.1$), of course, our approximation of incorporating only the adjacent wells breaks down.

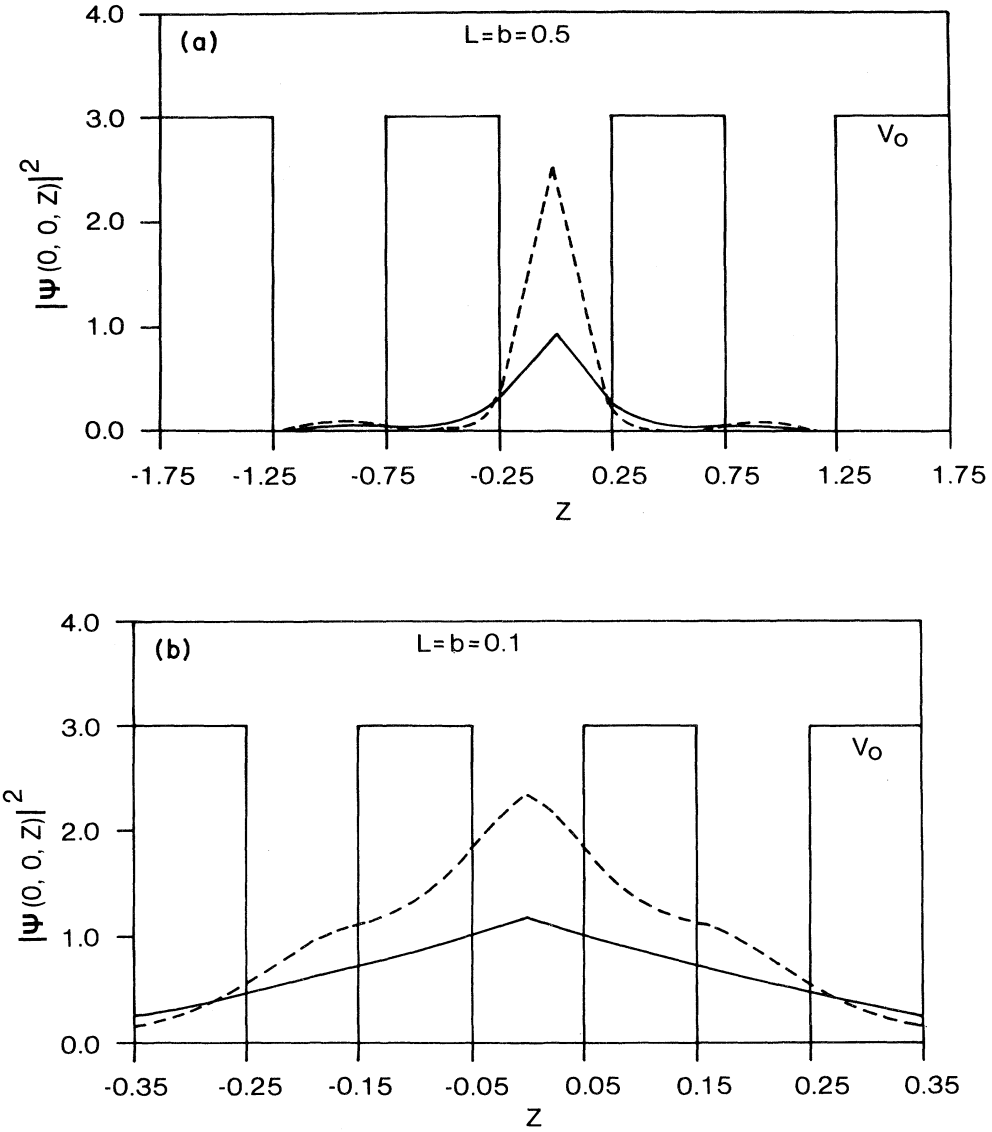

FIG. 4. Square of the wave function $|\Psi(0, 0, Z)|^2$ in arbitrary units vs position along the axis normal to the interfaces. Solid and dashed curves are for alloy compositions, $x=0.1$ and 0.4, respectively, of $Ga_{1-x}Al_xAs$. (a) and (b) are for equal GaAs and $Ga_{1-x}Al_xAs$ layer thicknesses $L=b=0.5$ and 0.1, respectively.

IV. SUMMARY AND DISCUSSION

We have calculated the ground-state-energy spectrum of hydrogenic-impurity atoms with respect to the first subband in GaAs-$Ga_{1-x}Al_xAs$ multiple-quantum wells. Variations of the ground-state binding energy of an impurity atom at the center of the quantum well are studied as a function of the well thickness as well as the barrier thickness. Wave functions are plotted for some typical values of well and barrier thicknesses.

To see how good the simple-product-type function [Eq. (7)] is as the trial function, we have compared our results in the single-well limit ($b=\infty$) with those of GB, whose wave functions containing a large number variational parameters are expanded in a Gaussian-type basis set. The binding energies of their calculation are found to differ from ours only by less than 4%. With the simplicity of the present wave function containing only a single variational parameter, it may be considered a good trial function.

We have neglected in our model the contributions arising from the difference in the effective masses and the dielectric constants in the two semiconductors and from the image forces.[1] By neglecting these contributions GB obtain binding energies which differ from those of MCM by only a few percent. The present calculation gives binding energies in the single-well limit less than those of GB by $\lesssim 4\%$ but very close to those of MCM. The reason that our results are close to those of MCM in this limit, even though we do not use different material parameters

and do not include image forces, may be that the binding energies obtained by the simple-product-type trial functions are (at most) a few percent less than those obtained by the trial functions of GB (and possibly of MCM with equal parameters for the two semiconductors) and this reduction happens to be close to the contributions arising from the different material parameters and image forces. Thus, in the single-well limit, the above-mentioned contributions are at most a few percent. Since, for thin superlattices, more wave functions are in GaAs than in the $Ga_{1-x}Al_xAs$ compared to single-well systems, these contributions may be even smaller. As the wells come closer to each other in a real multiple—quantum-well system, the subband levels are broadened gradually to form mini bands. But since our model consists of only three wells, we have neglected this effect. Although in principle one should include this broadening as well as the effects mentioned earlier to perform a calculation which should be valid for very thin superlattices, we feel that for superlattices with realistic dimensions the present model should be valid to predict the main features of the problem.

At present we cannot compare our results with any experiment, although there exists an experimental study of the variation of binding energy as a function of the well thickness.[10] The impurity was an acceptor, probably carbon. For carbon, the binding energy differs substantially (~ 14 meV) from that predicted by HEMT. So, first of all, our results which are valid only for hydrogenic impurities cannot be compared with experimental values. Secondly, even if the acceptor is assumed to be hydrogenic, since the well sizes were greater than $\sim 2.5a^*$, the binding energies corresponding to a multiple-quantum well are approximately equal to those corresponding a single well. However, we believe that with thin superlattices of dimensions available at present, it should be possible to see the variations in binding energy as a function of well or barrier thickness predicted by the present calculation. Because of the small effective electronic mass the multiple-well effects would be more pronounced for donors than for acceptors.

ACKNOWLEDGMENTS

We wish to thank Dr. K. K. Bajaj and Dr. D. C. Look for valuable discussions and comments. This work was performed at the Avionics Laboratory, Wright-Patterson Air Force Base, Dayton, Ohio under Contract No. F33615-81-c-1406.

APPENDIX

The transcendental Eq. (6) is obtained from the matching conditions at $z=a$, namely,

$$\cos(\alpha a)=Ae^{\beta a}+Be^{-\beta a},\quad -\alpha\sin(\alpha a)=\beta Ae^{\beta a}-\beta Be^{-\beta a}. \tag{A1}$$

The ratio A/B as a function of α and β is obtained from the wave-function matching conditions at other interfaces as

$$\begin{bmatrix} C \\ D \end{bmatrix}=\frac{Fe^{-\beta(3a+b)}}{\alpha}\begin{bmatrix} \alpha\cos[\alpha(3a+b)]+\beta\sin[\alpha(3a+b)] \\ \alpha\sin[\alpha(3a+b)]-\beta\cos[\alpha(3a+b)] \end{bmatrix},$$

$$\begin{bmatrix} A \\ B \end{bmatrix}=\frac{e^{\beta(a+b)}}{2\beta}\begin{bmatrix} \beta e^{-2\beta(a+b)} & e^{-2\beta(a+b)} \\ \beta & -1 \end{bmatrix}\begin{bmatrix} \cos[\alpha(a+b)] & \sin[\alpha(a+b)] \\ -\alpha\sin[\alpha(a+b)] & \alpha\cos[\alpha(a+b)] \end{bmatrix}\begin{bmatrix} C \\ D \end{bmatrix}. \tag{A2}$$

Solving Eq. (6) for E_0, the coefficients for the wave function are calculated from Eqs. (A1) and (A2). The integrals involved in the normalization and the expectation value of the Hamiltonian are defined as the following:

$$I_n(\alpha)=\left\{\frac{e^{-2z/\lambda}}{\Delta}\left[-\left[z+\frac{4}{\lambda\Delta}\right]\cos(2\alpha z)+\left[\alpha\lambda z+\frac{4\alpha}{\Delta}+\frac{\alpha\lambda^2}{2}\right]\sin(2\alpha z)\right]\right\}_{z=z_n}^{z=z_{n+1}}, \tag{A3}$$

where z_n and z_{n+1} are the lower and the upper z-coordinate values of the nth and $(n+1)$th regions, respectively (e.g., for $n=0$, $z_0=0$, $z_1=a$, etc.). The quantity Δ is defined as

$$\Delta=4(\alpha^2+1/\lambda^2), \tag{A4}$$

$$J_n(\beta)=\frac{\lambda}{2}\left[e^{2(\beta\lambda-1)z/\lambda}\left[\frac{z\lambda}{2(\beta\lambda-1)}+\frac{\lambda^2}{4}\frac{\beta\lambda-2}{(\beta\lambda-1)^2}\right]\right]_{z=z_n}^{z=z_{n+1}}, \tag{A5}$$

$$K_n(\alpha)=I_n\begin{bmatrix} \cos\to\sin \\ \sin\to-\cos \end{bmatrix}. \tag{A6}$$

The last equation means that $K_n(\alpha)$ is obtained from $I_n(\alpha)$ by replacing cos by sin and sin by $-\cos$ in $I_n(\alpha)$. We have

$$L_n(\alpha)=\frac{\lambda}{2\Delta}\left\{e^{-2z/\lambda}\left[-\left[\frac{2z}{\lambda}+\frac{4/\lambda^2-4\alpha^2}{\Delta}\right]\cos(2\alpha z)+\left[2\alpha z+\frac{8\alpha/\lambda}{\Delta}\right]\sin(2\alpha z)\right]\right\}_{z=z_n}^{z=z_{n+1}}, \tag{A7}$$

$$M_n(\alpha)=L_n\begin{bmatrix}\cos\rightarrow\sin\\ \sin\rightarrow-\cos\end{bmatrix}, \tag{A8}$$

$$P_n(\beta)=\frac{\lambda}{4(\beta-1/\lambda)}\left[e^{2(\beta-1/\lambda)z}\left[z-\frac{1}{2(\beta-1/\lambda)}\right]\right]_{z=z_n}^{z=z_{n+1}}, \tag{A9}$$

$$Q_n(\alpha)=\frac{\lambda}{2\Delta}\left[e^{-2z/\lambda}\left[-\frac{2\cos2\alpha z}{\lambda}+2\alpha\sin(2\alpha z)\right]\right]_{z=z_n}^{z=z_{n+1}}, \tag{A10}$$

$$R_n(\alpha)=Q_n\begin{bmatrix}\cos\rightarrow\sin\\ \sin\rightarrow-\cos\end{bmatrix}, \tag{A11}$$

$$S_n(\beta)=\frac{\lambda}{4(\beta-1/\lambda)}(e^{2(\beta-1/\lambda)z})_{z=z_n}^{z=z_{n+1}}. \tag{A12}$$

[1]C. Mailhiot, Y.-C. Chang, and T. C. McGill, Phys. Rev. B 26, 4449 (1982), and references therein.

[2]G. Bastard, Phys. Rev. B 24, 4714 (1981).

[3]R. L. Greene and K. K. Bajaj, Solid State Commun. 45, 825 (1983).

[4]H. C. Casey and M. B. Panish, *Heterostructure Lasers* (Academic, New York, 1978), Pt. A.

[5]S. T. Pantelides, Rev. Mod. Phys. 50, 797 (1978).

[6]H. J. Lee, L. Y. Juravel, J. C. Wooley, and A. J. Springthorpe, Phys. Rev. B 21, 659 (1980).

[7]T. Ando and S. Mori, J. Phys. Soc. Jpn. 47, 1518 (1977).

[8]J. N. Schulman and Y.-C. Chang, Phys. Rev. B 24, 4445 (1981); T. Ando and S. Mori, Surf. Sci. 113, 124 (1982).

[9]Q.-G. Zhu and H. Kroemer, Phys. Rev. B 27, 3519 (1983).

[10]R. C. Miller, A. C. Gossard, W. T. Tsang, and O. Monteanu, Phys. Rev. B 25, 3871 (1982).